Electrical Power and Energy Systems 56 (2014) 9–18

Contents lists available at ScienceDirect

Electrical Power and Energy Systems

journal homepage: www.elsevier.com/locate/ijepes

Recursive implementation of MUSIC algorithm to minimize power system disturbances

A. Elnady [a,b,*], A. Massoud [c], A. Noureldin [d]

[a] Electrical and Computer Engineering Department, University of Sharjah, P.O. Box 27272, Sharjah, United Arab Emirates
[b] (Adjunct) Electrical and Computer Engineering Department, Royal Military College, Station Forces, P.O. Box 17000, Kingston, Ontario K7K 7B4, Canada
[c] Queens University, Kingston, Ontario K7L 3N6, Canada
[d] Electrical and Computer Engineering Department, Royal Military College, Station Forces, P.O. Box 17000, Kingston, Ontario K7K 7B4, Canada

ARTICLE INFO

Article history:
Received 30 January 2013
Received in revised form 15 September 2013
Accepted 12 October 2013

Keywords:
Recursive root-MUSIC
Frequency tracking
Notch filter
Disturbance extraction and power systems

ABSTRACT

This paper exhibits new recursive implementation of the root-MUSIC algorithm in power system applications in order to extract the instantaneous power disturbances, which emanate from the arc furnace. The MUSIC algorithm is selected because it has an outstanding capability to estimate and track the frequencies of all types of distortion such as harmonics and interharmonics. The utilized algorithm has been newly developed so as to recursively track the instantaneous disturbances in the arc furnace current and consequently mitigate them. The suggested development of the recursive root-MUSIC is compared with the ESPRIT in order to prove that the adopted technique outperforms the high-resolution common techniques in a noisy or non-noisy environment. The instantaneous disturbance is formed by an innovative formulation of the recursive notch filter. Moreover, the experimental results are given to prove the practicality of the proposed concepts and techniques.

1. Introduction

Voltage and current disturbances are so common in power systems because the industrial distribution systems have numerous non-linear loads, which inject power disturbances. The disturbances of power systems encompass many power quality problems such as harmonics, interharmonics, voltage sags and flicker. Recently, interharmonics have gained much popularity because of their proliferation in industrial power systems. Therefore, there is an urgent need to estimate, track and even mitigate these harmonics and interharmonics in order to enhance the operation of power systems [1].

Tracking of the interharmonics has not been widely investigated in the past few decades because their frequencies are not known beforehand. In addition, these interharmonics cannot be predicated because they emanate from non-linear stochastic loads. Estimation of interharmonics depends mainly on the estimation of their frequencies. Some techniques have been developed to track the frequencies, magnitudes and phases of interharmonics [1–19]. Prony method has been used for frequency estimation under the existence of noise [2,3]. The Gauss–Newton algorithm is utilized to detect interharmonics parameters [4,5]. Wavelet transform is also employed for harmonics and interharmonics detection [6]. Discrete Fourier transform, along with its derivatives, has been developed based on IEC 61000-4-7 to estimate the frequencies of harmonics [7–9]. Two different versions of the least square techniques have been introduced to estimate the frequencies of disturbances in power systems [10]. Singular Value Decomposition, SVD, is being introduced for the frequency estimation in power systems [11]. Kalman filtering and its derivatives have been formulated for estimation of the frequency for distorted signals [12,13]. Min-Norm method has been proposed for interharmonics estimation, and it is proven that it gives better results than Prony method and FFT [14]. Adaptive notch filters have been recently used to estimate and extract frequencies of power disturbances [15,16]. High-resolution estimation techniques such as ESPRIT and MUSIC have been adopted to estimate the stationary (constant), frequencies in the off-line mode for power disturbances [17,18]. A new sinusoidal-tracking algorithm is developed to track the magnitudes and frequencies of interharmonics [19].

Some of the aforementioned techniques suffer from few shortcomings. The Gauss–Newton algorithm [4] depends greatly on the initial values for its estimation accuracy. FFT of [7–9] does not give accurate results if the estimated frequency is not located in the center of the subbands of estimated frequencies. Wavelet transform, [6], cannot be used for the instantaneous disturbance extraction in a real-time mode. The singular value decomposition, [11], is more mathematically complicated than FFT. Formulation of

* Corresponding author at: University of Sharjah, P.O. Box 27272, Sharjah, United Arab Emirates.
E-mail address: ayelnady71@gmail.com (A. Elnady).

0142-0615/$ - see front matter © 2013 Elsevier Ltd. All rights reserved.
http://dx.doi.org/10.1016/j.ijepes.2013.10.017

Kalman filtering to estimate the frequency [12] (which requires the complex extended Kalman filters), is mathematically too difficult to estimate several components. The algorithm presented in [19] is complicated since it requires demodulation and several filtering circuits before it can be applied.

The focus in this paper is being given to the recursive implementation of the subspace high-resolution techniques such as ESPRIT and MUSIC. The authors' survey reveals that the recursive implementation of high-resolution techniques is rare in power systems. In the last few years, ESPRIT has been reasonably used for stationary frequency estimation in the off-line mode [18,20,21]. The recursive implementation of ESPRIT is given in [18], where the recursion is realized by applying a sliding window concept. The width of widow (number of samples in data set), greatly affects the accuracy of the steady-state and transient performance for the estimation of frequencies, magnitudes and phases of the distorted signal. MUSIC is not as widely used as ESPRIT for frequency estimation in power systems [17,22], and it is only implemented to estimate a stationary (constant), distorted signal in the off-line mode.

The motivation for the research in this paper is to recursively utilize the root-MUSIC for estimation and tracking the injected variable disturbances of the arc furnaces in the industrial distribution systems. Moreover, the results of MUSIC for frequency estimation is fed to a new recursive notch filter for instantaneous disturbance extraction. The performance of MUSIC is compared with ESPRIT for the frequency estimation of the arc furnace current to prove that the novel recursive implementation of MUSIC gives the same accuracy as ESPRIT; and sometimes it outperforms ESPRIT in some cases. This paper consists of six sections. The second section illustrates the recursive implementation of MUSIC. The third section manifests the performance of the developed root-MUSIC compared to ESPRIT for frequency estimation in the noisy and non-noisy environment. The four section demonstrates the extraction of real arc furnace disturbances. The simulation and experimental results for the mitigation of the arc furnace disturbances are depicted in the fifth section. The last section summarizes the findings of this paper.

2. Recursive formulation for MUSIC

In this section, the formulation of the root-MUSIC is based on the basic algorithm given in [17,22]. The distorted signal, $x(t)$, for voltage and/or current at any sampling time t is expressed as,

$$x(t) = \sum_{k=1}^{P} A_k \cos(\omega_k t + \varphi_k) + e(t) \tag{1}$$

where A_k, ω_k, φ_k are the magnitude, frequency and phase for each sinusoid, $e(t)$ represents the corrupting additive zero-mean noise with variance σ, and P is the total number of component of interest (it should be determined beforehand). The set of data might be limited to length M samples, and this number is important for the recursive implementation as will be discussed later, but M should be greater than 2 P [17]. The set of samples can be defined as follows:

$$Samples = [\, x(t) \quad x(t+1) \quad \dots \quad x(t+M-1) \,] \tag{2}$$

by using the trigonometric function, the formula of (1) for any distortion component d_k at sample $t+n$ can be rewritten as,

$$d_k = A_k \cos(\omega_k n)\cos(\omega_k t + \varphi_k) - A_k \sin(\omega_k n)\sin(\omega_k t + \varphi_k) \tag{3}$$

the model for M samples observation vector can be written as,

$$x(t) = B(\omega)s(t) + e(t) \tag{4}$$

where

$$B(\omega) = [A(\omega_1), A(\omega_2), \dots, A(\omega_P)] \tag{5}$$

$$A(\omega_k) = \begin{bmatrix} \cos(\omega_k * 0) & \sin(\omega_k * 0) \\ \cos(\omega_k * 1) & \sin(\omega_k * 1) \\ \vdots & \vdots \\ \cos(\omega_k * (M-1)) & \sin(\omega_k * (M-1)) \end{bmatrix} \tag{6}$$

$$s(t) = \begin{bmatrix} A_1 \cos(\omega_1 t + \varphi_1) \\ A_1 \sin(\omega_1 t + \varphi_1) \\ \vdots \\ A_P \cos(\omega_P t + \varphi_P) \\ A_P \sin(\omega_P t + \varphi_P) \end{bmatrix} \tag{7}$$

The autocorrelation matrix R_x of the observation vector $x(t)$ is given as,

$$R_x = E\{x(t)x^T(t)\} = B(\omega)R_s B^T(\omega) + \sigma^2 I_M \tag{8}$$

where

$$R_s = E\{s(t)s^T(t)\} \tag{9}$$

I_M is the identity matrix of $M \times M$ dimension. The singular value decomposition can be implemented to eigen-decomposition as expressed by

$$R_x = \sum_{k=1}^{M} \lambda_k u_k u_k^T = U_S \sum_S U_S^T + U_N \sum_N U_N^T \tag{10}$$

where

$$\begin{aligned} U_S &= [u_1, \dots, u_{2P}] \\ U_N &= [u_{2P+1}, \dots, u_M] \end{aligned} \tag{11}$$

$$\sum_S = \begin{bmatrix} \lambda_1 & 0 & 0 & \dots & 0 \\ 0 & \lambda_2 & 0 & \dots & 0 \\ & & \vdots & & \\ 0 & 0 & 0 & \dots & \lambda_{2P} \end{bmatrix} \tag{12}$$

$$\sum_N = \begin{bmatrix} \lambda_{2P+1} & 0 & 0 & \dots & 0 \\ 0 & \lambda_{2P+2} & 0 & \dots & 0 \\ & & \vdots & & \\ 0 & 0 & 0 & \dots & \lambda_M \end{bmatrix} \tag{13}$$

where $\sum_S$, $\sum_N$ are the eigen values in the signal subspace and noise subspace, respectively. Any real-value of MUSIC algorithm is defined as,

$$p(\omega) = \frac{1}{f(\omega)} = \frac{1}{tr[A^T(\omega)U_N U_N^T A(\omega)]} \tag{14}$$

where $tr[\cdot]$ denotes the matrix trace operator. The peaks of $p(\omega)$ represent the zeros of denominator of (14). The frequencies can be calculated from (14) to the number of frequencies of interest.

The recursive implementation of the previous algorithm is implemented using the concept of sliding window since the vector of (2) is iteratively updated by a certain number of samples S, and the previous algorithm (from (2) to (14)), can be re-applied on a new updated data vector. There is a tradeoff between the number of updated samples S and the transient performance for frequency tracking or the computational burden for real-time evaluation; meaning that a less number of S yields fast tracking for frequencies; on the other side, a great number of S leads to more computational burden in the recursive estimation.

3. Testing the proposed formulation for the root-MUSIC algorithm

In this section, the proposed formulation of the root-MUSIC algorithm, along with the sliding window ESPRIT [18], is being applied to a non-noisy and noisy current fluctuation in order to check the steady-state and dynamic performance for the constant-frequency (stationary), and variable-frequency arc furnace current. This section is split into three parts; the first part exhibits the performance of MUSIC and ESPRIT for constant-frequency estimation in a non-noisy environment. The second part shows variable-frequency estimation in a non-noisy environment, while the last part demonstrates the same performance in a noisy environment.

3.1. Steady-state performance of root-MUSIC and ESPRIT for non-noisy current fluctuation

The test signal represents a primary-side current stemming from the arc furnaces, in which different kinds of harmonics are existent such as interharmonics and subharmonics. The test fluctuation current is expressed as,

$$\begin{aligned} I_{fluctuation} = {} & 500\sin(2\pi 50 + 0.3) + 30\sin(2\pi 15 + 0.27) + 10 \\ & \times \sin(2\pi 25 + 0.22) + 30\sin(2\pi 33 + 0.2) + 15 \\ & \times \sin(2\pi 47 + 0.5) + 35\sin(2\pi 79 + 0.34) + 30 \\ & \times \sin(2\pi 95 + 0.66) + 15\sin(2\pi 113 + 0.27) + 25 \\ & \times \sin(2\pi 205 + 0.52) + 75\sin(2\pi 250 + 0.2) + 55 \\ & \times \sin(2\pi 350 + 0.22) \end{aligned} \quad (15)$$

The performance of MUSIC and ESPRIT for the frequency estimation is demonstrated in this section. For all these techniques, the concept of sliding window is applied to track the frequencies as demonstrated in the second section. The window size for ESPRIT is 300 samples with a sampling frequency of 1 kHz, and the window size for MUSIC can be reduced down to 150 samples with the same sampling frequency of 1 kHz. The data set is shifted by one sample at a time. Fig. 1 shows the performance of the developed root-MUSIC, ESPRIT [18], Recursive Gauss–Newton [4] and FFT [7,8]. Apparently, both MUSIC and ESPRIT (subspace high-resolution techniques), have very accurate estimation, which matches with the results given in [14]. While, Gauss–Newton and FFT (state-space estimation techniques), do not give as accurate results as the high-resolution techniques. ESPRIT and MUSIC performance is depicted in Fig. 1a and b. The recursive Gauss–Newton, Fig. 1c, does not give accurate estimation to three frequencies (47 Hz, 79 Hz and 95 Hz); in addition to its awkward transient performance as shown in Fig. 1c. Whereas, FFT is utilized based on 5-Hz frequency resolution as given in IEC 61000-4-7 [7,8]. The harmonic spectrum of FFT is portrayed in Fig. 1d, in which two frequencies (33 Hz and 113 Hz), are not accurately detected because of the common drawbacks of FFT mentioned in [19]. In conclusion, the performance of the subspace high-resolution techniques is much better than the state-space estimation techniques as illustrated and proved through Fig. 1. Consequently, for the rest of this paper the performance of recursive MUSIC is given in comparison with ESPRIT as an efficient technique for frequency estimation.

3.2. Dynamic performance of root-MUSIC and ESPRIT for non-noisy current fluctuation

This part investigates the dynamic (transient), performance for the recursive implementation of MUSIC and ESPRIT. The test signal has a change in the frequency of three components at $t = 0.45$ s. The new current fluctuation is given in (16), at which 47 Hz becomes 40 Hz, 95 Hz goes to 80 Hz and 205 Hz is changed to 215 Hz.

$$\begin{aligned} I_{fluctuation} = {} & 500\sin(2\pi 50t + 0.3) + 30\sin(2\pi 15t + 0.27) \\ & + 10\sin(2\pi 25t + 0.22) + 30\sin(2\pi 33t + 0.2) \\ & + 15\sin(2\pi 40t + 0.5) + 35\sin(2\pi 79t + 0.34) \\ & + 30\sin(2\pi 80t + 0.66) + 15\sin(2\pi 113t + 0.27) \\ & + 25\sin(2\pi 215t + 0.52) + 75\sin(2\pi 250t + 0.2) \\ & + 55\sin(2\pi 350t + 0.22) \end{aligned} \quad (16)$$

The dynamic performance is influenced by the sampling frequency, the width of data set, M, and the number of the shift samples for a sliding window S. A faster dynamic performance stems from a higher sampling frequency and smaller shift samples S and vice versa. The window width, sampling frequency and shift samples are selected as 100 samples, 1 kHz and 1 sample, respectively for the following waveforms of Fig. 2. Aforementioned numbers are arbitrary selected to have an optimum dynamic performance for both techniques. Fig. 2 demonstrates this dynamic performance for both techniques when the fluctuation current changes from (15) to (16) at $t = 0.45$. This figure affirms that MUSIC and ESPRIT almost has the same dynamic performance, while ESPRIT has a bigger overshoot than MUSIC.

3.3. Performance of MUSIC and ESPRIT for a noisy fluctuation current

In this subsection, both techniques will be applied on a noisy arc furnace current for different SNRs. The test current of (15) is distorted by different SNRs, the resultant current is applied to both techniques. Fig. 3 exhibits the frequency estimation of both techniques when the current is distorted by a SNR of 10 dB. Also, it reveals that MUSIC has a bad transient performance and meritorious steady-state performance since it is less sensitive to the noise than ESPRIT.

The steady-state estimated frequencies are given in Table 1 to show the accuracy of MUSIC compared to ESPRIT for the distorted current of (15) at $t = 0.55$ s. The values of the estimated frequencies are given in Table 1 to show the accuracy of MUSIC compared to ESPRIT for a heavily distorted current of (15) at $t = 0.55$ s.

Finally, it is noteworthy mentioning that MUSIC does not have as good dynamic performance as ESPRIT, but it has better steady state performance for a wide range of the signal-to-noise ratio. Aforementioned attribute favors MUSIC over ESPRIT for the power quality disturbance extraction because the power disturbances have a domination of low-frequency harmonics rather than high-frequency harmonics.

4. Extraction of the arc furnace disturbance by the proposed MUSIC algorithm

The previous section demonstrates the estimation capability of MUSIC for a distorted signal. In this section, the proposed formulation is being applied to a real power quality disturbance, which is embedded in the arc furnace current. The arc furnace is modeled by a non-linear time-variable arc resistance, where its performance is very accurate and similar to the real arc furnace [23]. This model is programmed and integrated in the system under study using MATLAB/SIMULINK, which is shown in Fig. 4; this system is part of an industrial real distribution system in US [24]. The developed recursive MUSIC algorithm is utilized in order to estimate the dominant frequencies and track the instantaneous current disturbance. This section is split into two subsections; the first subsection shows the application of the recursive MSUIC to estimate and track

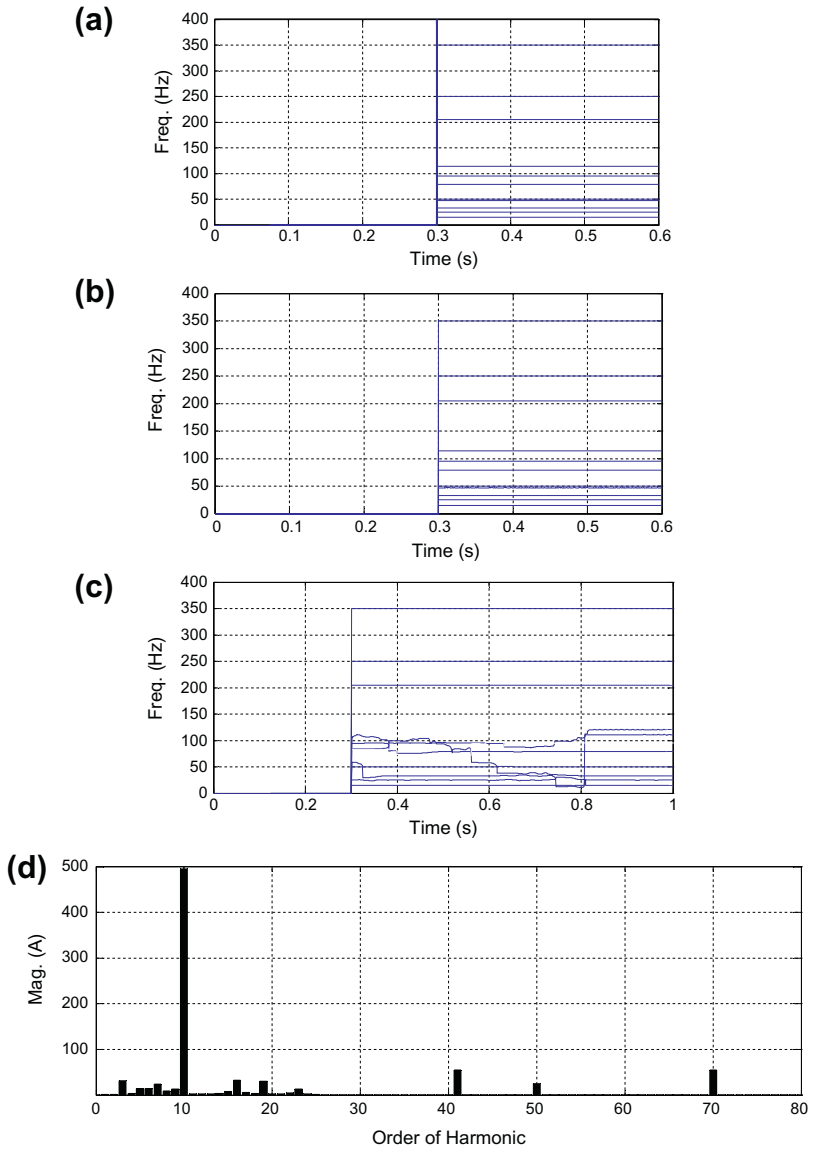

Fig. 1. Steady-state frequency estimation for both techniques: (a) ESPRIT, (b) MUSIC, (c) Gauss_Newton, and (d) FFT based on 5-Hz frequency resolution.

the frequencies of the disturbances, and the second subsection demonstrates the tracking of the instantaneous disturbance signals.

4.1. Frequency estimation for the arc furnace current

The arc furnace is intentionally selected because it is known that the arc furnace is a non-linear variable load whose injected disturbances are too difficult to be tracked because its disturbances encompass different harmonics (characteristic and non-characteristic), interharmonics and subharmonics.

The arc furnace current at the primary side of the arc transformer for one phase, I_{arc} as depicted in the system of Fig. 4, is given in Fig. 5a, the details for the same current is given in Fig. 5b to clearly show the distortion of this current, and the estimated frequencies are portrayed in Fig. 5c. The estimated frequencies are limited to the ten dominant components, these frequencies look reasonable because they match the typical frequencies of the injected disturbances of real arc furnaces as published in [25]. The estimated frequencies for these ten dominant components are given as,

$$f = \begin{bmatrix} 36.0274 & 49.9989 & 62.8973 & 134.5767 & 149.4573 \\ 161.2211 & 249.9769 & 255.3677 & 349.5846 & 449.7181 \end{bmatrix} \quad (17)$$

4.2. Disturbance tracking for the arc furnace current

The extraction of the instantaneous disturbance can be done after the estimation of disturbance frequencies. There are several techniques that have been introduced to extract the disturbance signals [26–28]. In this research, the notch filter is adopted and its recursive implementation is developed to extract and detect the fundamental component, individual disturbance component and the total disturbances [26]. The notch filter is innovatively formulated in this work because it has several advantages over some other state-estimation techniques [27–29] such as,

1. Its ability to track any component within the distortion without knowing the total number of components within this distorted signal.

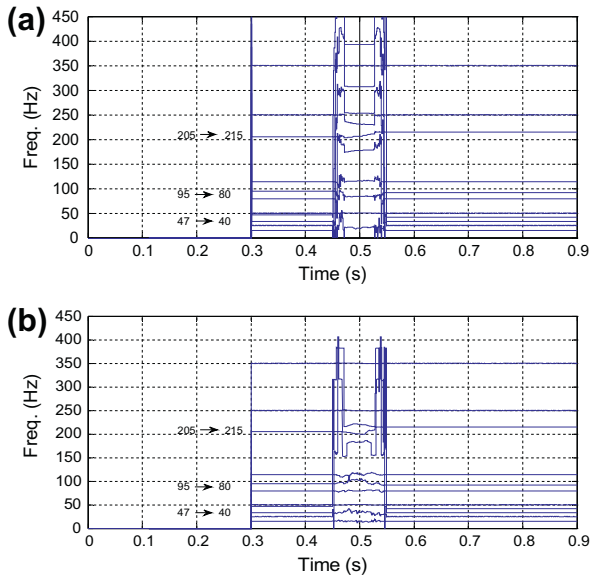

Fig. 2. Transient performance for both techniques due to frequency changes: (a) ESPRIT and (b) MUSIC.

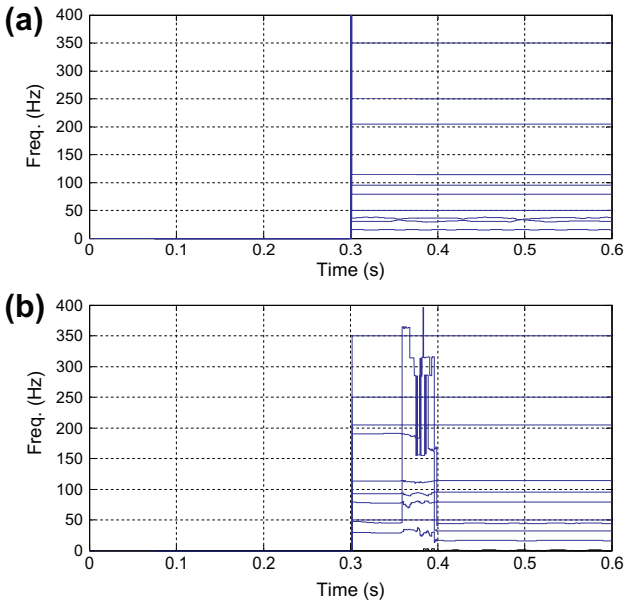

Fig. 3. Frequency estimation in a noisy environment: (a) ESPRIT and (b) MUSIC.

Table 1
Comparison between MUSIC and ESPRIT for steady-state estimation of frequencies of (1) with SNR of 10 dB and 30 dB at $t = 0.55$ s.

Estimated freq.	MUSIC		ESPRIT	
	10 dB	30 dB	10 dB	30 dB
50	49.99	49.98	50.01	49.99
15	16.67	16.14	16.10	16.75
25	0.19	23.45	1000.00	22.76
33	32.29	33.30	32.10	32.33
47	44.28	44.31	36.00	44.99
79	79.00	78.99	79.01	78.99
95	95.00	94.99	95.00	95.00
113	113.75	113.75	113.80	113.75
205	205.00	205.00	205.00	205.00
250	250.00	250.00	250.00	250.00
350	350.00	350.00	350.00	350.00

2. If the notch frequency is not accurately estimated, the proper selection of the bandwidth can alleviate this inaccuracy and the same component can be suppressed accurately.
3. Its mathematical formulation for recursive estimation is easy.
4. The formulation of the recursive notch filter (to extract the disturbance signal), starts with defining the continuous-domain transfer function of this filter as,

$$H(s) = \frac{S^2 + f_n^2}{S^2 + b_\omega S + f_n^2} \tag{18}$$

where f_n and b_ω are the notch filter frequency and bandwidth, respectively. By using the bi-linear transformation, the expression of (18) can be rewritten in the discrete-domain function as follows:

$$H(z) = \frac{(1+f_n^2) - (1-f_n^2)z^{-1} + (1+f_n^2)z^{-2}}{(1+f_n^2+b_\omega) - 2(1-f_n^2)z^{-1} + (1+f_n^2-b_\omega)z^{-2}} \tag{19}$$

this transfer function is rewritten and simplified in the discrete-time domain as,

$$H(z) = \frac{1}{2} * \frac{(1+a_2)z^2 - 2a_1 z^1 + (1+a_2)}{z^2 - a_1 z^1 + a_2} \tag{20}$$

where

$$a_1 = \frac{2(1-f_n^2)}{1+f_n^2+b_\omega}, \quad a_2 = \frac{1+f_n^2-b_\omega}{1+f_n^2+b_\omega}$$

The recursive formulation for the notch filter can be adopted to instantaneously extract any disturbance even if its frequency is not precisely known in advance. As mentioned before, the proper selection of the filter bandwidth can alleviate this pitfall. To realize this objective the recursive state-estimation can be written as,

$$\begin{aligned} x(t+1) &= A(t)x(t) + B(t)u(t) \\ y(t) &= C(t)x(t+1) + D(t)u(t) \end{aligned} \tag{21}$$

where $y(t)$ is the output of the notch filter, which represents the whole signal without the signal that has been suppressed. If it is required to extract a specific signal with a notch frequency f_n, the output of the filter $y(t)$ is subtracted from the input $u(t)$. The coefficients of (21) for the controllable discrete realization for the discrete transfer function are given as,

$$\begin{aligned} A(t) &= \begin{bmatrix} a_1 & -a_2 \\ 1 & 0 \end{bmatrix} \\ B(t) &= \begin{bmatrix} 1 \\ 0 \end{bmatrix} \\ C(t) &= \begin{bmatrix} \frac{a_1}{2}(a_2 - 1) & \frac{1-a_2^2}{2} \end{bmatrix} \\ D(t) &= \frac{1+a_2}{2} \end{aligned} \tag{22}$$

The recursive formulation of (21) is used to extract the instantaneous reference current, which is equal to the total disturbance ($I_{ref.}$ of Fig. 4 = $I_{\text{total-disturbance}}$). The block diagram that illustrates the total and/or any individual disturbance extraction is presented in Fig. 6 by using the recursive notch filter formulated in Eqs. (18)–(21).

The proposed formulation is applied on the arc furnace current of Fig. 5a to instantaneously extract the fundamental component, some specific disturbances with particular frequencies and the total disturbances as described and illustrated in Fig. 6. Formulation of (21) and (22) can be used to track any particular disturbance with a known frequency and the total disturbances as shown in Fig. 7a–d.

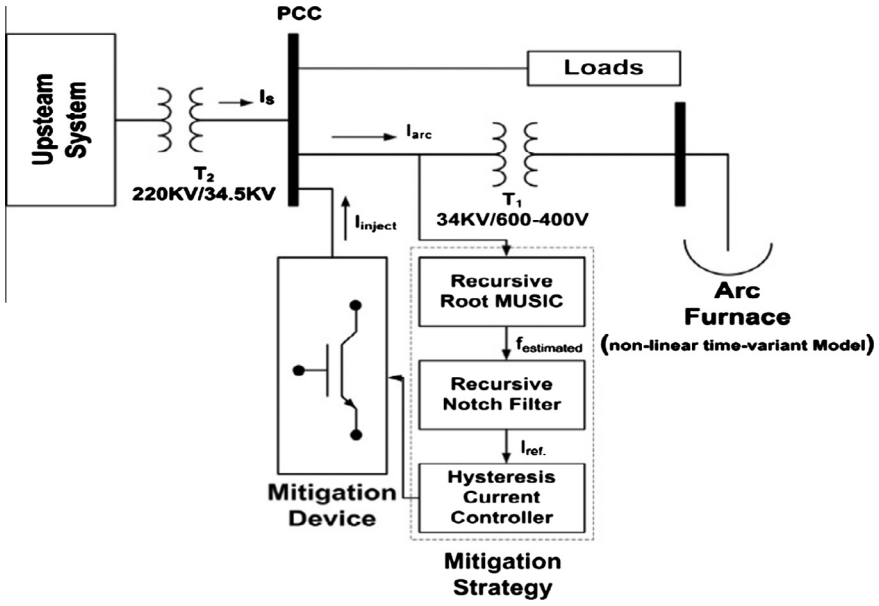

Fig. 4. Block diagram for the arc furnace integrated with the system under study.

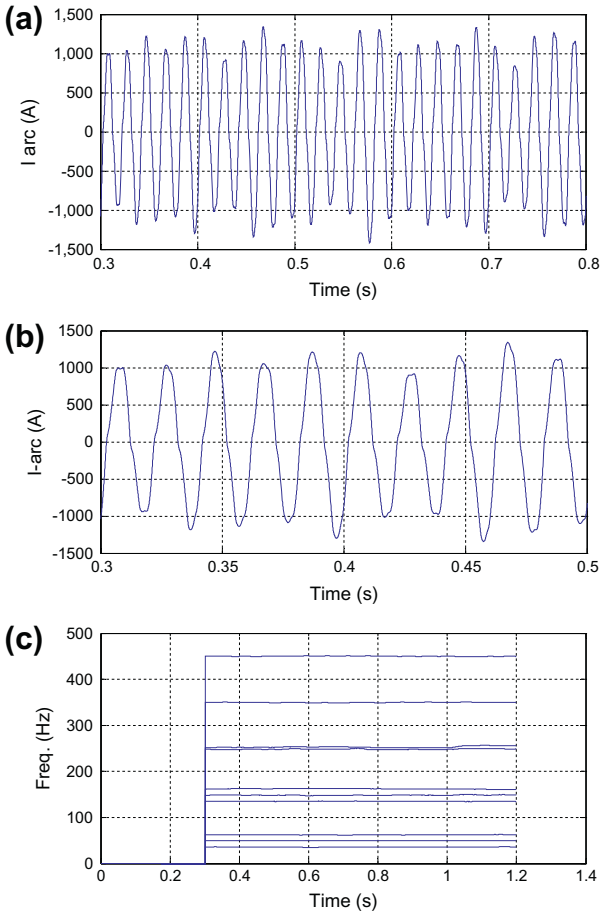

Fig. 5. Estimation for the frequencies for the disturbances in the arc furnace current: (a) The arc furnace current. (b) Zooming-in for the arc furnace current from time 0.3 s to 0.5 s. (c) Estimation of frequencies of the arc furnace current.

The waveforms of Fig. 7 reveal important point about the arc furnace current, which encompasses variable disturbances and a variable fundamental current taken by the arc furnace. This

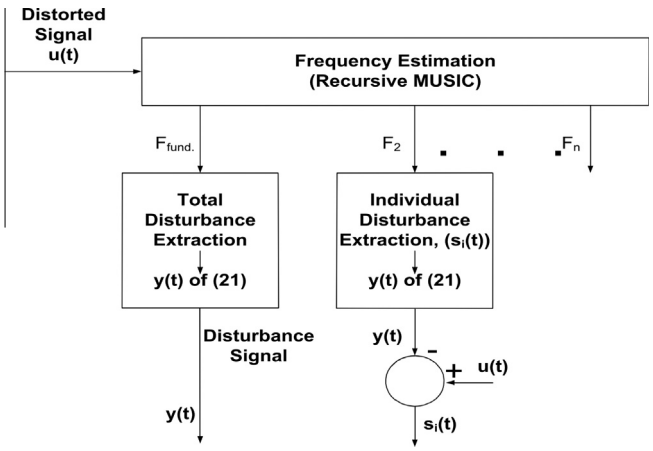

Fig. 6. Block diagram for total and/or any individual disturbance extraction.

operational characteristic greatly matches the performance of real arc furnaces [30]. The variation in the fundamental and disturbances result from the arc furnace model that depends on a nonlinear time-variable arc resistance [23].

5. Mitigation of the power system disturbances

Mitigation of disturbances can be realized if the disturbance extraction is accurate and fast enough. In this section, recursive MUSIC and notch filter are developed to extract the instantaneous disturbances as shown in the previous sections. In this section, the arc furnace (as a source of disturbances), is selected because it is considered as the most difficult load from disturbance estimation, tracking and mitigation prospective in industrial distribution systems. Two simulation cases will be demonstrated; the first case represents the arc furnace current with stationary frequencies, while the second case shows an arc furnace current with variable frequencies. Finally, two experimental cases are given to show the implementation of the recursive developed technique for the mitigation of different harmonics and interharmonics distortion.

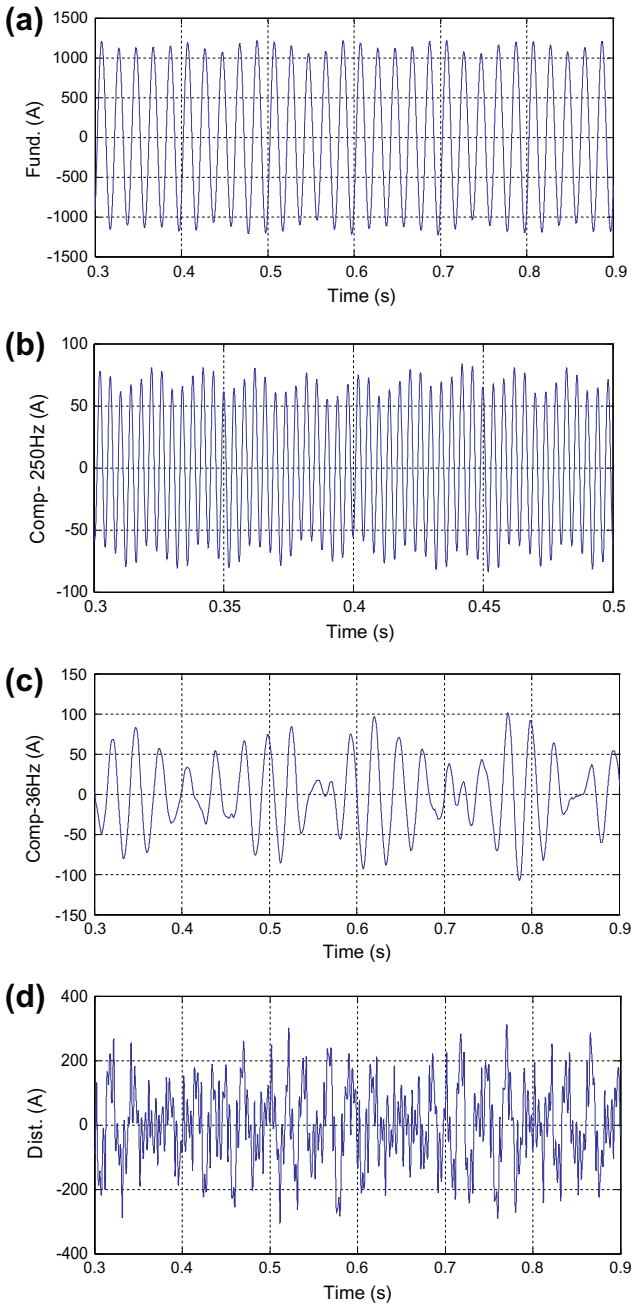

Fig. 7. The instantaneous extraction of some components of the arc furnace current: (a) Fundamental component. (b) Disturbance of 250 Hz. (c) Disturbance of 36 Hz. (d) Total disturbance of the arc furnace current.

5.1. Mitigation of the arc furnace current with stationary frequencies

As mentioned earlier, this section shows the mitigation of the distorted current of Fig. 5a. The mitigation is realized using the extracted instantaneous disturbance of Fig. 7d, which is implemented to operate the shunt mitigation device of Fig. 4. The mitigated current is illustrated in Fig. 8, where Fig. 8a shows the mitigated current, I_s, and Fig. 8b is just zooming for the waveform of Fig. 8a.

The comparison between Figs. 7a and 8a indicates the accuracy of the mitigation process since the two waveforms represent the same fundamental current and they match each other; meaning that the source current becomes just the fundamental component and all harmonic distortion has been eradicated. Similarly, the comparison between Figs. 5b and 8b affirms the accuracy of the

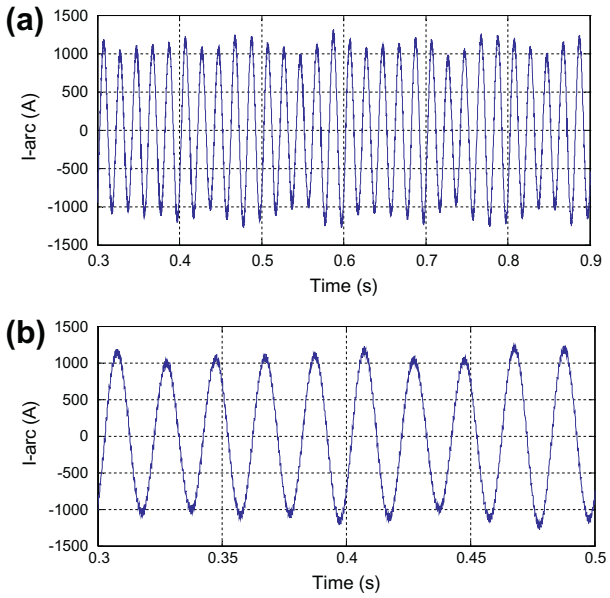

Fig. 8. The mitigated arc furnace current: (a) The source current I_s (mitigated current). (b) Detailed waveform of Fig. 7a for a time from 0.3 s to 0.5 s.

disturbance extraction because the disturbances embedded in Fig. 5b have been eliminated in Fig. 8b, and the current (at source side), is just a pure sinusoidal component superimposed on high-frequency noise emanating from the switching action of the mitigation device. Finally, the accuracy of the mitigation process is mathematically validated by the THD for the source current before and after the mitigation, which is reduced from 9.5% to 5.1%.

5.2. Mitigation of the arc furnace current with variable frequencies

The expression of the arc resistance of the arc model has been changed at $t = 1$ s. As a result, some magnitudes and frequencies will be changing at that time. The arc current, given in Fig. 9, depicts the current before and after the transition at $t = 1$ s. The estimated frequencies before this transition are already given in (17); while the new estimated frequencies, after this transition, are given as,

$$f = \begin{bmatrix} 30.8346 & 49.9125 & 69.2666 & 133.6461 & 149.6800 \\ 167.7940 & 233.5690 & 249.7553 & 255.0188 & 349.3234 \end{bmatrix} \quad (23)$$

The mitigation of the arc furnace current is displayed in Fig. 10. The mitigated current indicates almost the fundamental component only, which proves the accuracy of the disturbance extraction and mitigation.

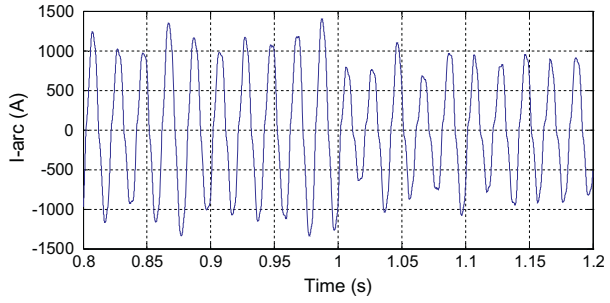

Fig. 9. Arc furnace current with variable magnitudes and variable frequencies.

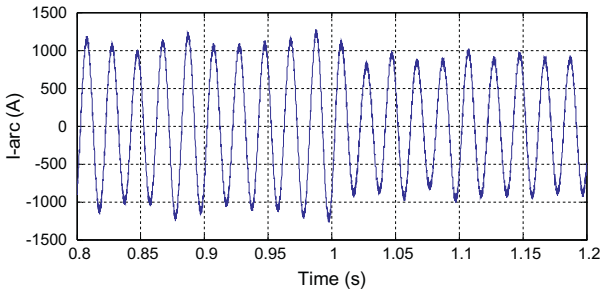

Fig. 10. Arc furnace current after the mitigation.

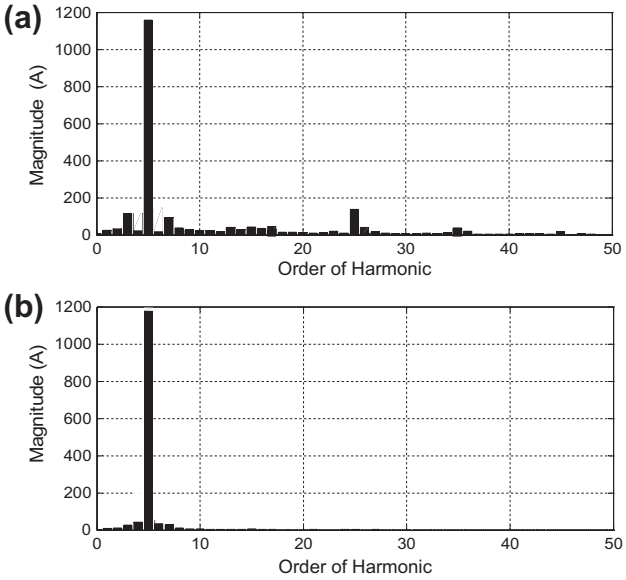

Fig. 11. Harmonic spectrum before and after the mitigation at time = 1.2 s: (a) Spectrum before mitigation. (b) Spectrum after mitigation.

The efficiency of disturbance extraction is verified through displaying the harmonic spectrum before and after the mitigation as portrayed in Fig. 11 with a base frequency of 10 Hz. The THD after the mitigation is 5.2%.

5.3. Experimental results for the mitigation of different distorted currents

This subsection demonstrates the practical implementation of the recursive notch filter (formulated from (18) to (22)), to experimentally extract and mitigate the disturbance of different distorted current. This subsection is split into two parts. The first part demonstrates how the proposed technique is used to extract and compensate for the characteristic (regular), harmonics; while the second part illustrates the ability of the proposed technique to detect and mitigate the interharmonics. The hardware setup is depicted as a block diagram in Fig. 12 for the rating of 0.5 kV A, the data for experimental setup are given below,

- A platform for programming notch filter is an evaluation DSP board TI-320LF2407.
- A voltage source converter of power MOSFETs-IRF 830 operated in a current controlled mode.
- A Hysteresis Current Controller (HCC), with 20% hysteresis band to regulate the output current, the details of operation and structure of the HCC are given in [31].
- A programmable AC power source-Chroma 61500 to generate current waveform.
- A current transducer is LEM 25NP.

The recursive notch filter is programmed in this DSP board with a notch filter of 50 Hz and bandwidth of 5 Hz. The extracted disturbance is equal to the output of the notch filter as explained in Fig. 6.

The first part of this subsection shows how the suggested extraction technique is used to extract the regular harmonic disturbances. Fig. 13 depicts a square-waveform current, which is generated by the programmable AC source. This waveform is applied on the recursive notch filter, which is developed in the DSP board to extract all disturbances, the disturbance current waveform is also given in the same figure. Both waveforms have a current scale of 1 A/div. The distorted current is illustrated in the upper waveform, and the extracted disturbance is given in the lower waveform.

The extracted disturbance is employed to generate the injected current in order to kill its disturbance. The extracted, lower waveform, current along with the injected current, upper waveform, are given in Fig. 14. Both waveforms have a current scale of 1 A/div.

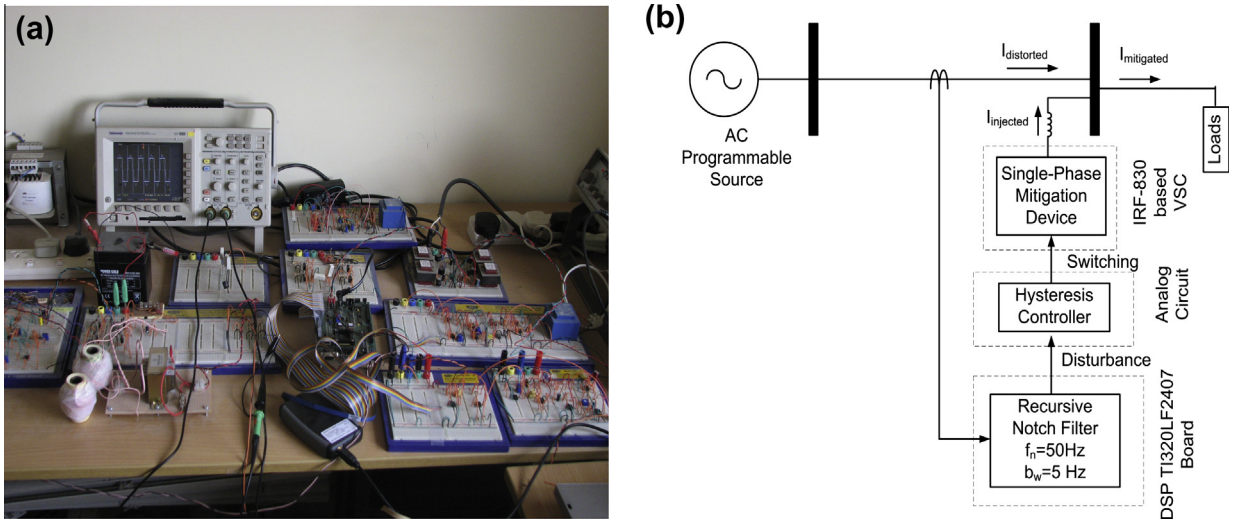

Fig. 12. Experimental setup and its block diagram: (a) A picture for the experimental setup. (b) Block diagram for the experimental setup.

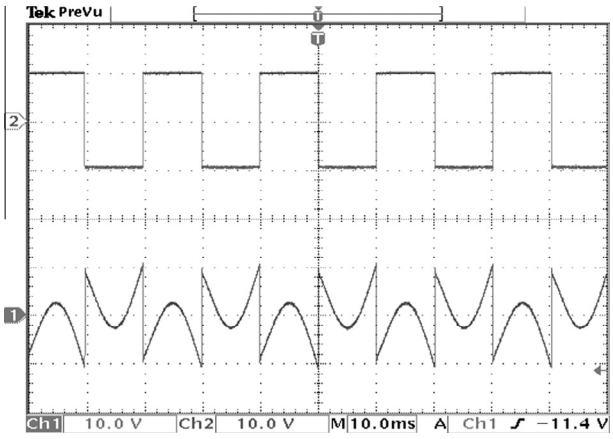

Fig. 13. Square-waveform distorted current (upper waveform), and extracted disturbances (lower waveform).

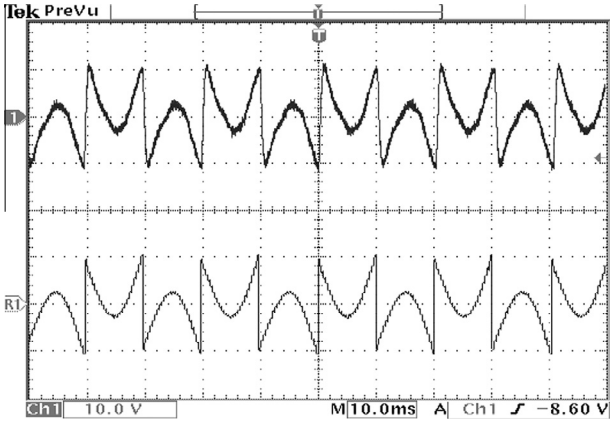

Fig. 14. The injected (upper waveform) and reference (lower waveform), current waveforms.

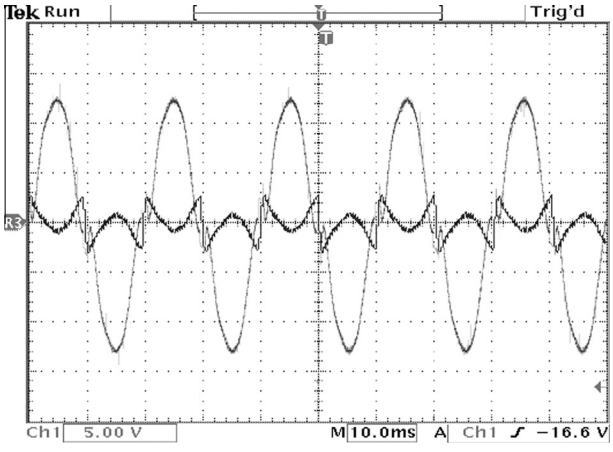

Fig. 15. Mitigated (bigger waveform), and injected (smaller waveform), current waveforms.

The mitigated current waveform is given in Fig. 15, where the mitigated current along with the same injected current are displayed. The mitigated current has a scale of 0.5 A/div. and the injected current has a scale of 2 A/div.

The second part of this subsection clarifies the ability of the propounded technique to detect the interharmonics. The distorted current is represented by the waveform in Fig. 16, where this waveform represents a sinusoid distorted by interharmonics, and its scale is 1 A/div. The mitigated current and the injected current are given in Fig. 17, the first waveform is the mitigated current with a scale of 1 A/div., and the second waveform is the injected current with a scale of 0.5 A/div. This injected current results from the operation the hysteresis current controller, which receives the disturbance from the proposed formulation for the extraction techniques as explained in Section 4.

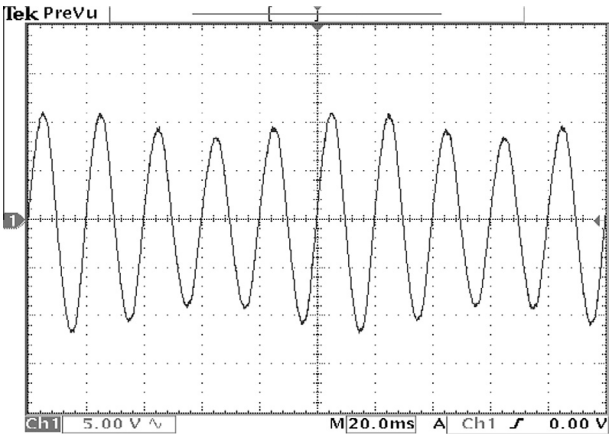

Fig. 16. Distorted current waveform by interharmonics.

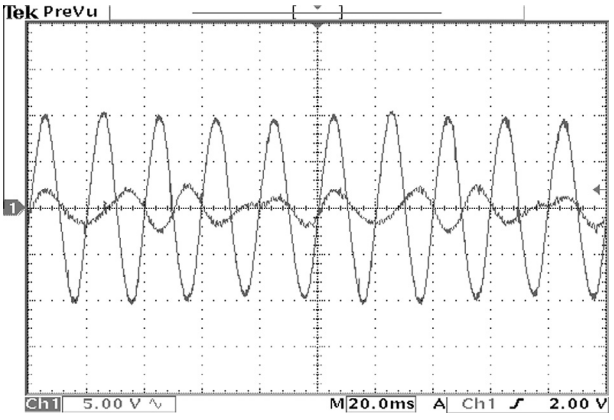

Fig. 17. Mitigated (bigger waveform), and injected (smaller waveform), current waveforms for interharmonics disturbance.

6. Conclusion

This paper introduces a recursive implementation of MUSIC in power systems since the MUSIC algorithm has been developed and utilized in an iterative manner to estimate the constant and variable frequencies of power system disturbances and consequently track the individual and total instantaneous power disturbances. The proposed formulation of MUSIC is proved to have as the same performance as ESPRIT for the stationary and dynamic frequency estimation in a noisy and non-noisy environment as indicated in the presented waveforms and tables. The presented results affirm that MUSIC has better steady state estimation than ESPRIT for a wide range of the signal-to-noise ratio. Moreover, the developed MUSIC and the presented recursive notch filter are efficiently utilized for frequency estimation and disturbance extraction of a real arc furnace current. The efficiency of the disturbance extraction and mitigation process is validated by calculating

the THD and displaying the harmonic spectrum before and after the mitigation process, where the THD is reduced from 9.5% to 5.1%. Eventually, the experimental results are given based on a prototype system of 0.5 kV A to prove the practicality of the proposed disturbance extraction technique.

References

[1] Chen CI, Liu YJ, Wu MC. Measuring power system harmonics and interharmonics by an improved fast Fourier transform-based algorithm. Proc IET Gener Transm Distrib 2008;2:193–201.

[2] Hauer JF, Demeure CJ, Scharf LL. Initial results in Prony analysis of power systems response signals. IEEE Trans Power Syst 1990;5:80–9.

[3] Lobos T, Rezmer J. Real-time determination of power system frequency. IEEE Trans Instrum Meas 1997;46:877–81.

[4] Abatzoglou TJ. A fast maximum likelihood algorithm for frequency estimation of a sinusoid based on Newton's method. IEEE Trans Acoust Speech Signal Process 1985;33:77–89.

[5] Stoica P, Moses RL, Friedlander B, Soderstorm T. Maximum likelihood estimation of the parameters of multiple sinusoids from noisy measurements. IEEE Trans Acoust Speech Signal Process 1989;37:378–91.

[6] Morsi WG, El-Hawary ME. Suitable mother wavelet for harmonics and interharmonics measurements using wavelet packet transform. In: Proc Canadian conference electrical and computer engineering; 2007. p. 748–52.

[7] Yang JZ, Liu CW. A precise calculation of power system frequency. IEEE Trans Power Deliv 2001;16:361–6.

[8] Cheng Lin H. Power harmonics and interharmonics measurement using recursive group-harmonic power minimizing algorithm. IEEE Trans Ind Electron 2012;59:1184–93.

[9] Saini MK, Kapoor R. Classification of power quality events – a review. Int J Electr Power Energy Syst – Elsevier 2012;1:11–9.

[10] Subudhi B, Panda AM, Mohanty SR. Parameter estimation techniques applied to power networks. Proc TENCON 2008:1–5.

[11] Osowski S. SVD technique for estimation of harmonic components in a power system. Proc IEE Gener Transm Distrib 1994;141:473–9.

[12] Huang CH, Lee CH, Shih KJ, Wang YJ. Frequency estimation of distorted power system signals using a robust algorithm. IEEE Trans Power Deliv 2008;23:41–51.

[13] Abdelsalam AA, Eldesouky AA, Sallam AA. Classification of power system disturbances using linear Kalman filter and fuzzy expert system. Int J Electr Power Energy Syst – Elsevier 2012;43:688–95.

[14] Lobos T, Leonoaicz Z, Rezmer J, Schegner P. High resolution spectrum estimation methods for signal analysis in power systems. IEEE Trans Instrum Measur 2006;55:1–8.

[15] Karimi-Ghartemani M, Iravani MR. Measurement of harmonics/inter-harmonics of time-varying frequency. IEEE Trans Power Deliv 2005;20:23–31.

[16] Ketabi A, Farshadnia M, Malekpour M, Feuillet R. A new control strategy for active power line conditioner (APLC) using adaptive notch filter. Int J Electr Power Energy Syst – Elsevier 2013;47:31–40.

[17] Leonowicz Z, Lobos T. Parametric spectral estimation for power quality assessment. In: Proc international conference on computer as a tool EUROCON; 2007. p. 1641–7.

[18] Gu IYH, Bollen MHJ. Estimating interharmonics by using sliding-window ESPRIT. IEEE Trans Power Deliv 2008;23:13–23.

[19] Schenne ML, Ziarani AK, Ortmeyer TH. A novel adaptive flicker measurement technique. Int J Electr Power Energy Syst – Elsevier 2011;10:1686–94.

[20] Jain SK, Singh SN. Exact model order ESPRIT technique for harmonics and interharmonics estimation. IEEE Trans Instrum Measur 2012;61:1915–23.

[21] Bracale A, Carpinelli G. An ESPRIT and DFT-based new method for the waveform distortion assessment in power. In: Proc 20th electricity distribution; 2009. p. 430–4.

[22] Cai T, Duan S, Liu B, Liu F, Chen C. Real-value MUSIC algorithm for power harmonics and interharmonics estimation. Int J Circuit Theory Appl 2010;39:1023–35.

[23] Zheng T, Makram EB. An adaptive arc furnace model. IEEE Trans Power Deliv 2001;15:931–9.

[24] Andrews D, Bishop MT, Witte JF. Harmonic measurements, analysis, and power factor correction in a modern steel manufacturing facility. IEEE Trans Ind Appl 1996;32:617–24.

[25] Testa A, Akram MF, Burch R, Carpinelli G, Chang G, Dinavahi V, et al. Interharmonics: theory and modeling. IEEE Trans Power Deliv 2007;22:2335–49.

[26] Elnady A, Noureldin A. Mitigation of arc furnace voltage flicker using an innovative of adaptive notch filters. IEEE Trans Power Deliv 2011;26:1326–36.

[27] Marei MI, Abdel-Galil TK, El-Saadany EF. Hilbert transform based control algorithm of the DG interface for voltage flicker mitigation. IEEE Trans Power Deliv 2005;20:1129–33.

[28] Soliman SA, El-Hawary ME. Measurement of power systems voltage and flicker levels for power quality analysis: a static LAV state estimation based algorithm. Int J Electr Power Energy Syst – Elsevier 2000;22:447–50.

[29] Mojiri M, Karimi-Ghartemani M, Bakhshai A. Time-domain signal analysis using adaptive notch filter. IEEE Trans Signal Process 2007;55:85–93.

[30] Understanding Electric Arc Furnace Operation. Technical report. <http://infohouse.p2ric.org/ref/10/09047.pdf>.

[31] Panda G, Ray PK, Puhan PS, Dash SK. Novel schemes used for estimation of power systems harmonics and their elimination in a three-phase distribution system. Int J Electr Power Energy Syst – Elsevier 2013;53:842–56.